SLAC – PUB – 3416
August 1984
T/E

POLARIZED HADRONIC COLLISIONS: QCD AND TEST OF ELECTROWEAK GAUGE MODELS*

MASUD CHAICHIAN

Department of High Energy Physics, University of Helsinki, Helsinki, Finland

MASAKI HAYASHI†

Stanford Linear Accelerator Center

Stanford University, Stanford, California, 94305

JACQUES SOFFER

Centre de Physique Théorique, CNRS, Luminy, F-13288 Marseille, France

KENJI YAMAGISHI‡

Stanford Linear Accelerator Center

Stanford University, Stanford, California, 94305

Submitted to *Physical Review* **D**

* Work supported by the Department of Energy, contract DE – AC03 – 76SF00515.

† Permanent address: Department of Physics, Saitama Medical College, Saitama 350-04, Japan.

‡ Permanent address: Department of Physics, Tokuyama University, Yamaguchi 745, Japan.

Abstract

Lowest order QCD is applied for the angular distributions of high-mass dileptons with large transverse momentum produced in reactions, $\bar{p}p, pp \to (\gamma^*, Z_1^0, Z_2^0, ...) + X \to \ell^+\ell^- + X$ with longitudinally polarized proton beam(s). General formulas, which are applicable to any gauge model of the underlying electroweak interactions, are given. Numerical results are presented for the angular distributions in $\bar{p}p$ and pp collisions at $\sqrt{s} = 540$ GeV for the CERN $\bar{p}p$ collider and $\sqrt{s} = 2$ TeV for the Fermilab Tevatron within the standard model and the left-right model, which is also consistent with existing data. Signals which could distinguish between the different electroweak gauge models are revealed.

1. Introduction

The standard $SU(2) \times U(1)$ electroweak model of Glashow, Weinberg and Salam[1] has been quite successful in all respects including the predictions for the gauge bosons, $W^{\pm}$ and Z^0, which have been experimentally found at the CERN $\bar{p}p$ collider.[2] However, there exist other electroweak models which differ from the standard one, but in low energy region coincide with it.[3] Such models, besides other considerations, emerge also from some grand unified theories and thus have their own *raison d'être*.[4] Therefore, it is of considerable interest to study such models on the same footing as the standard one and look for their experimental verifications. One such method is the detailed study of the angular distributions of the dileptons produced in the hadron-hadron collisions. To carry out the most detailed study we start with the polarized proton beams, especially since such experiments are feasible and are under consideration. The case of unpolarized hadronic reactions, of course, come out as a special case.

Many authors[5–9] have studied the polarization effects for the gauge bosons $W^{\pm}$ and Z^0 production and their decay into lepton pairs in polarized hadronic collisions. The polarization effects in the hadronic decays of $W^{\pm}$ have been studied in Ref[10]. On the basis of such studies it has been emphasized that the experiments with a polarized proton beam would provide a variety of useful information, supplementing those of unpolarized collisions[11–14] on the underlying electroweak interactions and the production mechanism of their gauge bosons. Further, a recent study has indicated that polarized proton beams at intensities close to the ordinary intensity of unpolarized beams are attainable with the new technology.[15]

In this paper we calculate and discuss the angular distributions of high-mass dileptons produced with large transverse momentum in high energy polarized and unpolarized hadronic collisions. Because of restriction to such a kinematical region, we have all the right to utilize the lowest order ,i.e., $O(\alpha_s)$ perturbative QCD which has been proven to describe quite successfully similar processes.[16] We consider the reactions

$$\bar{p}p, pp \to (\gamma^*, Z_1^0, Z_2^0, ...) + X \to \ell^+\ell^-(\ell = e \quad \text{or} \quad \mu) + X, \qquad (1.1)$$

where the proton beam p is (or both pp are) longitudinally polarized. The present work is the extension of our previous one[14] in which the case of unpolarized beams has been studied within the standard electroweak model. Here we consider polarized beams and aim at other tests which can distinguish between the standard Glashow-Weinberg-Salam and the left-right electroweak models. A short account of this work has previously been reported.[17] Kinnunen and Lindfors[7] have also studied the angular distributions for ℓ^+ produced in the reaction with the longitudinally polarized proton beam p_h with a helicity h

$$\bar{p}p_h \to (\gamma^*, Z^0) + X \to \ell^+\ell^- + X,$$

in the rest system of Z^0 at $M = M_Z$. We differ from their study in that, whilst they restrict themselves to the Drell-Yan mechanism and to the standard model, we consider the first order QCD processes (dilepton production with large transverse momentum) and also consider the comparisons of the predictions of the standard and the left-right models. Also unlike in Ref. 6, we will not use the 3-quarks SU(6) wave function model for the spin dependent structure functions.

In Section 2 we present all the basic formulas for the reactions (1.1) for the general electroweak models. Section 3 presents two electroweak models we have considered, namely the standard and the left-right ones, together with the parametrization for the polarized parton distributions. Section 4 is devoted to the numerical results for differential cross-sections and the polarization asymmetries for the coefficients in the angular distribution. Section 5 contains the conclusion.

2. Basic Formulas

The Lagrangian for the neutral-current interaction reads as:

$$\mathcal{L}_{int} = e\bar{\ell}\gamma_\mu \ell A^\mu + \sum_i C_i \bar{\ell}\gamma_\mu (a_i^\ell - b_i^\ell \gamma_5)\ell Z_i^\mu + \sum_i C_i \bar{f}\gamma_\mu (a_i^f - b_i^f \gamma_5) f Z_i^\mu, \quad (2.1)$$

where A_μ, ℓ, f and Z_i^0 $(i = 1, 2, ...)$ are the photon, lepton, quark with flavour f, and $i-$th neutral gauge boson field, respectively. a_i and b_i (a_i^f and b_i^f) denote the vector and axial-vector coupling constants of the lepton (quark f) to the Z_i^0-boson. These couplings and the parameters C_i which depend on the gauge group under consideration will be specified in the next section.

In the lowest order of QCD perturbation theory the angular distributions of high-mass(M) lepton pairs produced with large transverse momentum Q_T in reactions (1.1) are given by two hard parton processes: quark q-antiquark $\bar{q}$ annihilation into $(\gamma^*, Z_1^0, Z_2^0, ...)$ and a gluon G, and gluon-quark Compton scattering. The relevant Feynman diagrams are shown in Figs. 1a and 1b. We have calculated the differential cross-sections of the lepton pair from the decay of $(\gamma^*, Z_1^0, Z_2^0 ...)$ produced in polarized annihilation and Compton subprocesses at fixed M^2, $\hat{t}$ and a solid angle $\Omega_\ell^* = (\theta, \phi)$ of one of leptons in the dilepton rest-frame. The final formulas for these partonic differential cross-sections, assuming massless leptons and quarks, are presented below.

For the annihilation subprocess (denoted by A)

$$q(h_1) + \bar{q}(h_2) \to (\gamma^*, Z_1^0, Z_2^0, ...) + G \to \ell^+\ell^- + G \quad (2.2)$$

(h_1 is the helicity of the quark and h_2 is that of the antiquark), we obtain

$$\frac{d\hat{\sigma}_A(h_1,h_2)}{dM^2 d\hat{t} d\Omega_\ell^*} = \frac{d\hat{\sigma}_A}{dM^2 d\hat{t}}(unpol.)(1-h_1h_2)\frac{3}{16\pi}$$

$$\Big[\Big(1-\frac{h_1N_f}{K_f}\Big)\{1+\cos^2\theta+\hat{A}_0(\frac{1}{2}-\frac{3}{2}\cos^2\theta)+\hat{A}_1\sin 2\theta\cos\phi+\hat{A}_2\cdot\frac{1}{2}\sin^2\theta\cos 2\phi\}$$

$$+2(L_f-h_1M_f)/K_f\{\hat{A}_3\sin\theta\cos\phi+\hat{A}_4\cos\theta\}\Big]. \tag{2.3}$$

For the Compton scattering (denoted by C)

$$G(\Lambda)+q(h_1)\to(\gamma^*,Z_1^0,Z_2^0,...)+q\to\ell^+\ell^-+q \tag{2.4}$$

(Λ is the helicity of the gluon), we have

$$\frac{d\hat{\sigma}_C(\Lambda,h_1)}{dM^2 d\hat{t} d\Omega_\ell^*} = \frac{d\hat{\sigma}_A}{dM^2 d\hat{t}}(unpol.)\frac{3}{16\pi}$$

$$\Big[\Big(1-\frac{h_1N_f}{K_f}\Big)\{(1+h_1\Lambda\hat{B}_{00})(1+\cos^2\theta)+(\hat{A}_0+h_1\Lambda\hat{B}_0)(\frac{1}{2}-\frac{3}{2}\cos^2\theta)$$

$$+(\hat{A}_1+h_1\Lambda\hat{B}_1)\sin 2\theta\cos\phi+(\hat{A}_2+h_1\Lambda\hat{B}_2)\frac{1}{2}\sin^2\theta\cos 2\phi\} \tag{2.5}$$

$$+2(L_f-h_1M_f)/K_f\{(\hat{A}_3-h_1\Lambda\hat{B}_3)\sin\theta\cos\phi+(\hat{A}_4-h_1\Lambda\hat{B}_4)\cos\theta\}\Big],$$

where caret denotes quantities at the parton level. The coefficients $\hat{A}_i$ (which take the same form in both annihilation and Compton subprocesses), $\hat{B}_{00}$ and $\hat{B}_i(i=0,1,2,3,4)$ are functions of parton momenta $\mathbf{p}_1$ and $\mathbf{p}_2$ in the dilepton rest-system and read as:

$$\hat{A}_0=\hat{A}_2=\frac{p_{1x}^2+p_{2x}^2}{|\mathbf{p}_1|^2+|\mathbf{p}_2|^2},\qquad \hat{A}_1=\frac{p_{1x}p_{1z}+p_{2x}p_{2z}}{|\mathbf{p}_1|^2+|\mathbf{p}_2|^2},$$

$$\hat{A}_3 = \frac{|\mathbf{p}_1|p_{1x} - |\mathbf{p}_2|p_{2x}}{|\mathbf{p}_1|^2 + |\mathbf{p}_2|^2}, \qquad \hat{A}_4 = \frac{|\mathbf{p}_1|p_{1z} - |\mathbf{p}_2|p_{2z}}{|\mathbf{p}_1|^2 + |\mathbf{p}_2|^2},$$

$$\hat{B}_{00} = \frac{|\mathbf{p}_2|^2 - |\mathbf{p}_1|^2}{|\mathbf{p}_1|^2 + |\mathbf{p}_2|^2},$$

$$\hat{B}_0 = \hat{B}_2 = \frac{p_{2x}^2 - p_{1x}^2}{|\mathbf{p}_1|^2 + |\mathbf{p}_2|^2}, \qquad \hat{B}_1 = \frac{p_{2x}p_{2z} - p_{1x}p_{1z}}{|\mathbf{p}_1|^2 + |\mathbf{p}_2|^2},$$

$$\hat{B}_3 = \frac{|\mathbf{p}_1|p_{1x} + |\mathbf{p}_2|p_{2x}}{|\mathbf{p}_1|^2 + |\mathbf{p}_2|^2}, \qquad \hat{B}_4 = \frac{|\mathbf{p}_1|p_{1z} + |\mathbf{p}_2|p_{2z}}{|\mathbf{p}_1|^2 + |\mathbf{p}_2|^2}. \tag{2.6}$$

All informations about the underlying electroweak interactions are contained in K_f, L_f, M_f, and N_f:

$$K_f = \frac{e_f^2}{M^4} - 2\sum_i e_f(\frac{C_i}{e})^2 a_i a_i^f \frac{\mathrm{Re}D_i}{M^2} + 2\sum_{i<j}(\frac{C_iC_j}{e^2})^2$$

$$(a_ia_j + b_ib_j)(a_i^f a_j^f + b_i^f b_j^f)\mathrm{Re}(D_iD_j^*)$$

$$+ \sum_i (\frac{C_i}{e})^4 (a_i^2 + b_i^2)\{(a_i^f)^2 + (b_i^f)^2\}|D_i|^2,$$

$$L_f = -2\sum_i e_f(\frac{C_i}{e})^2 b_i b_i^f \frac{\mathrm{Re}D_i}{M^2} + 2\sum_{i<j}(\frac{C_iC_j}{e^2})^2$$

$$(a_ib_j + b_ia_j)(a_i^f b_j^f + b_i^f a_j^f)\mathrm{Re}(D_iD_j^*)$$

$$+ 4\sum_i (\frac{C_i}{e})^4 a_ib_ia_i^f b_i^f |D_i|^2,$$

$$M_f = -2\sum_i e_f(\frac{C_i}{e})^2 b_i a_i^f \frac{\mathrm{Re}D_i}{M^2} + 2\sum_{i<j}(\frac{C_iC_j}{e^2})^2$$

$$(a_ib_j + b_ia_j)(a_i^f a_j^f + b_i^f b_j^f)\mathrm{Re}(D_iD_j^*)$$

$$+ 2\sum_i (\frac{C_i}{e})^4 a_ib_i\{(a_i^f)^2 + (b_i^f)^2\}|D_i|^2,$$

$$N_f = -2\sum_i e_f(\frac{C_i}{e})^2 a_i b_i^f \frac{\mathrm{Re}D_i}{M^2} + 2\sum_{i<j}(\frac{C_i C_j}{e^2})^2$$

$$(a_i a_j + b_i b_j)(a_i^f b_j^f + b_i^f a_j^f)\mathrm{Re}(D_i D_j^*) \qquad (2.7)$$

$$+ 2\sum_i (\frac{C_i}{e})^4 (a_i^2 + b_i^2) a_i^f b_i^f |D_i|^2,$$

where D_i is the propagator of the Z_i^0-boson with its mass M_{Z_i} and the width Γ_{Z_i}:

$$D_i = (M^2 - M_{Z_i}^2 + iM_{Z_i}\Gamma_{Z_i})^{-1}. \qquad (2.8)$$

The differential cross-sections in the unpolarized case are[14] :

$$\frac{d\hat{\sigma}_A}{dM^2 d\hat{t}}(unpol.) = \frac{4}{9}\cdot\frac{2}{3}\frac{\alpha^2\alpha_s}{\hat{s}^2}\frac{(\hat{t}-M^2)^2 + (\hat{u}-M^2)^2}{\hat{t}\hat{u}}M^2 K_f,$$

$$\frac{d\hat{\sigma}_C}{dM^2 d\hat{t}}(unpol.) = \frac{1}{6}\cdot\frac{2}{3}\frac{\alpha^2\alpha_s}{\hat{s}^2}\frac{(\hat{s}-M^2)^2 + (\hat{u}-M^2)^2}{-\hat{s}\hat{u}}M^2 K_f. \qquad (2.9)$$

with the standard notations.

In order to calculate the cross-sections $d\sigma_{A,C}/dM^2 dy dQ_T^2$ (where y is the rapidity of the dilepton) and the coefficients $A_i (i = 0,1,2,3,4)$ in the angular distributions for the polarized hadronic collisions, one has to convolute the corresponding quantities for the subprocesses (i.e. the ones with caret) with the parton spin distribution functions inside the hadrons $f_{f(\pm)}^{p(+)}$, $G_\pm^+(x)$, etc. (e.g., $f_{f(\pm)}^{p(+)}$ and $G_\pm^+(x)$ denote the spin distribution functions of the valence quark f and the gluon G with the helicity ± 1 inside a proton with $h = +1$.) Then the differential cross-section for processes (1.1) can be expanded in terms of the

$\Omega_\ell^*(\theta,\phi)$ as:

$$\frac{d\sigma(h_1,h_2)}{dM^2dydQ_T^2d\Omega_\ell^*} \propto 1+\cos^2\theta + A_0(h_1,h_2)(\frac{1}{2}-\frac{3}{2}\cos^2\theta)$$
$$+ A_1(h_1,h_2)\sin 2\theta\cos\phi + A_2(h_1,h_2)\frac{1}{2}\sin^2\theta\cos 2\phi \qquad (2.10)$$
$$+ A_3(h_1,h_2)\sin\theta\cos\phi + A_4(h_1,h_2)\cos\theta.$$

[The formula for the angular distribution at the one-loop order have been derived in Ref.[18]] The total coefficients of the angular distributions can be obtained in an analogous way as in the unpolarized case, by summing over the annihilation and the Compton contributions, i.e.,

for $\bar{p}p_h-$collision with the helicity $h=\pm 1$

$$A_i(\pm) = \frac{A_i d\sigma_A(\pm) + A_i d\sigma_C(\pm)}{d\sigma(\pm)}, \qquad (i=0,1,2,3,4), \qquad (2.11)$$

where

$$d\sigma(\pm) = d\sigma_A(\pm) + d\sigma_C(\pm),$$

$$d\sigma_{A,C}(\pm) = d\sigma_{A,C}(\pm)/dM^2dydQ_T^2.$$

for p_hp_h-collision with the helicity $h=\pm 1$

$$A_i(\pm\pm) = \frac{A_i d\sigma_A(\pm\pm) + A_i d\sigma_C(\pm\pm)}{d\sigma(\pm\pm)}, \qquad (i=0,1,2,3,4), \qquad (2.12)$$

where

$$d\sigma(\pm\pm) = d\sigma_A(\pm\pm) + d\sigma_C(\pm\pm),$$

$$d\sigma_{A,C}(\pm\pm) = d\sigma_{A,C}(\pm\pm)/dM^2 dy dQ_T^2.$$

In the following we present the formulas derived assuming that the valence quark f and the gluon G are polarized, but the sea-quark component remains unpolarized in the proton.

for $\bar{p}p_h$ – collision

One can define the asymmetry of the $(1+\cos^2\theta)$ term of the cross-section (See Eq.(2.10)) due to the longitudinal beam polarization as

$$Asymmetry = \frac{d\sigma(-) - d\sigma(+)}{d\sigma(-) + d\sigma(+)} = \frac{\sum_f \{\Delta F^{p\bar{p}}(A) + \Delta F_{00}^{p\bar{p}}(C)\} N_f}{\sum_f \{F^{p\bar{p}}(A) + F^{p\bar{p}}(C)\} K_f}, \qquad (2.13)$$

where

$$\Delta F^{p\bar{p}}(A) = \Delta f_f^p(x_1) f_{\bar{f}}^{\bar{p}}(x_2) d\hat{\sigma}_A,$$

$$\Delta F_{00}^{p\bar{p}}(C) = \{-\Delta G(x_1) f_{\bar{f}}^{\bar{p}}(x_2) \hat{B}_{00} + \Delta f_f^p(x_1) G(x_2)\} d\hat{\sigma}_C,$$

$$F^{p\bar{p}}(A) = f_f^p(x_1) f_{\bar{f}}^{\bar{p}}(x_2) d\hat{\sigma}_A,$$

$$F^{p\bar{p}}(C) = \{G(x_1) f_{\bar{f}}^{\bar{p}}(x_2) + f_f^p(x_1) G(x_2)\} d\hat{\sigma}_C,$$

$$d\hat{\sigma}_{A,C} = d\hat{\sigma}_{A,C}/dM^2 d\hat{t},$$

$$\Delta f_f^p(x_1) = f_{f(+)}^{p(+)}(x_1) - f_{f(-)}^{p(+)}(x_1),$$

$$f_f^p(x_1) = f_{f(+)}^{p(+)}(x_1) + f_{f(-)}^{p(+)}(x_1). \qquad (2.14a)$$

(The similar formulas hold for $\Delta f_{\bar{f}}^{\bar{p}}(x_2)$ etc.)

$$\Delta G(x_1) = G_+^+(x_1) - G_-^+(x_1),$$

$$G(x_1) = G_+^+(x_1) + G_-^+(x_1). \qquad (2.14b)$$

From Eq. (2.13) it is clear that the sign of this asymmetry is related through N_f to that of the axial couplings b_i^f and this is the only way to determine it.

Also one can define the polarization (spin) asymmetries for the coefficients in the angular distributions:

$$\Delta A_i = \frac{A_i(-) - A_i(+)}{A_i(-) + A_i(+)}, \qquad (i = 0,1,2,3,4). \qquad (2.15a)$$

Writing in an explicit form we have for $i = 0,1,2$

$$\Delta A_i = \frac{\sum_f \{\Delta F_i^{p\bar{p}}(A) + \Delta F_i^{p\bar{p}}(C)\} N_f}{\sum_f \{F_i^{p\bar{p}}(A) + F_i^{p\bar{p}}(C)\} K_f}, \qquad (i = 0,1,2), \qquad (2.15b)$$

where

$$\Delta F_i^{p\bar{p}}(A) = \Delta f_f^p(x_1) f_{\bar{f}}^{\bar{p}}(x_2) \hat{A}_i d\hat{\sigma}_A, \qquad (i = 0,1,2,3,4),$$

$$\Delta F_i^{p\bar{p}}(C) = \{-\Delta G(x_1) f_{\bar{f}}^{\bar{p}}(x_2) \hat{B}_i + \Delta f_f^p(x_1) G(x_2) \hat{A}_i\} d\hat{\sigma}_C, \qquad (i = 0,1,2),$$

$$F_i^{p\bar{p}}(A) = f_f^p(x_1) f_{\bar{f}}^{\bar{p}}(x_2) \hat{A}_i d\hat{\sigma}_A, \qquad (i = 0,1,2,3,4),$$

$$F_i^{p\bar{p}}(C) = \{G(x_1) f_{\bar{f}}^{\bar{p}}(x_2) + f_f^p(x_1) G(x_2)\} \hat{A}_i d\hat{\sigma}_C, \qquad (i = 0,1,2,3,4),$$

Note that relations $A_0 = A_2$ and $\Delta A_0 = \Delta A_2$ hold on account of a $\mathbf{p}_1 \leftrightarrow \mathbf{p}_2$ symmetry, reflecting the vector nature of the gluon[19] (however, $A_0 \neq A_2$ and $\Delta A_0 \neq \Delta A_2$, if the gluon would appear to be a scalar particle).

For $i = 3, 4$ we have

$$\Delta A_i = \frac{\sum_f \{\Delta F_i^{p\bar{p}}(A) + \Delta F_i^{p\bar{p}}(C)\} M_f}{\sum_f \{F_i^{p\bar{p}}(A) + F_i^{p\bar{p}}(C)\} L_f}, \qquad (i = 3, 4), \tag{2.15c}$$

where

$$\Delta F_i^{p\bar{p}}(C) = \{\Delta G(x_1) f_{\bar{f}}^{\bar{p}}(x_2) \hat{B}_i + \Delta f_f^p(x_1) G(x_2) \hat{A}_i\} d\hat{\sigma}_C, \qquad (i = 3, 4).$$

$\underline{p_h p_h - \text{collision}}$

Similarly one can define various experimentally accessible polarization asymmetries when both of the proton beams are longitudinally polarized:

$$Asymmetry = \frac{d\sigma(--) - d\sigma(++)}{d\sigma(--) + d\sigma(++)}, \tag{2.16a}$$

which can be rewritten as

$$Asymmetry = \frac{\sum_f \{\Delta F^{pp}(A) + \Delta F_{00}^{pp}(C)\} N_f}{\sum_f \{F^{pp}(A) + F_{00}^{pp}(C)\} K_f}, \tag{2.16b}$$

where

$$\Delta F^{pp}(A) = \{\Delta f_f^p(x_1) f_{\bar{f}}^p(x_2) + f_{\bar{f}}^p(x_1) \Delta f_f^p(x_2)\} d\hat{\sigma}_A,$$

$$\Delta F_{00}^{pp}(C) = \{G(x_1) \Delta f_f^p(x_2) + \Delta G(x_1) f_f^p(x_2) \hat{B}_{00}\} d\hat{\sigma}_C,$$

$$F^{pp}(A) = \{f_f^p(x_1) f_{\bar{f}}^p(x_2) + f_{\bar{f}}^p(x_1) f_f^p(x_2)\} d\hat{\sigma}_A,$$

$$F_{00}^{pp}(C) = \{G(x_1) f_f^p(x_2) + \Delta G(x_1) \Delta f_f^p(x_2) \hat{B}_{00}\} d\hat{\sigma}_C.$$

For the polarization asymmetries of the coefficients in the angular distribution

we have

$$\Delta A_i = \frac{A_i(--) - A_i(++)}{A_i(--) + A_i(++)}, \qquad (i = 0,1,2,3,4). \tag{2.17a}$$

Explicitly for $i = 0,1,2$ we have

$$\Delta A_i = \frac{\sum_f \{\Delta F_i^{pp}(A) + \Delta F_i^{pp}(C)\} N_f}{\sum_f \{F_i^{pp}(A) + F_i^{pp}(C)\} K_f}, \qquad (i = 0,1,2), \tag{2.17b}$$

where

$$\Delta F_i^{pp}(A) = \{\Delta f_f^p(x_1) f_{\bar{f}}^p(x_2) + f_{\bar{f}}^p(x_1) \Delta f_f^p(x_2)\} \hat{A}_i d\hat{\sigma}_A, \qquad (i = 0,1,2),$$

$$\Delta F_i^{pp}(C) = \{G(x_1) \Delta f_f^p(x_2) \hat{A}_i + \Delta G(x_1) f_f^p(x_2) \hat{B}_i\} d\hat{\sigma}_C, \qquad (i = 0,1,2),$$

$$F_i^{pp}(A) = \{f_f^p(x_1) f_{\bar{f}}^p(x_2) + f_{\bar{f}}^p(x_1) f_f^p(x_2)\} \hat{A}_i d\hat{\sigma}_A, \qquad (i = 0,1,2),$$

$$F_i^{pp}(C) = \{G(x_1) f_f^p(x_2) \hat{A}_i + \Delta G(x_1) \Delta f_f^p(x_2) \hat{B}_i\} d\hat{\sigma}_C, \qquad (i = 0,1,2).$$

One has also $A_0 = A_2$ and $\Delta A_0 = \Delta A_2$, because of $\mathbf{p}_1 \leftrightarrow \mathbf{p}_2$ symmetry and the vector nature of the gluon.

For $i = 3,4$ we have

$$\Delta A_i = \frac{\sum_f \{\Delta F_i^{pp}(A) + \Delta F_i^{pp}(C)\} M_f}{\sum_f \{F_i^{pp}(A) + F_i^{pp}(C)\} L_f}, \qquad (i = 3,4), \tag{2.17c}$$

where

$$\Delta F_i^{pp}(A) = \{\Delta f_f^p(x_1) f_{\bar{f}}^p(x_2) - f_{\bar{f}}^p(x_1) \Delta f_f^p(x_2)\} \hat{A}_i d\hat{\sigma}_A, \qquad (i = 3,4),$$

$$\Delta F_i^{pp}(C) = \{G(x_1) \Delta f_f^p(x_2) \hat{A}_i - \Delta G(x_1) f_f^p(x_2) \hat{B}_i\} d\hat{\sigma}_C, \qquad (i = 3,4),$$

$$F_i^{pp}(A) = \{f_f^p(x_1) f_{\bar{f}}^p(x_2) - f_{\bar{f}}^p(x_1) f_f^p(x_2)\} \hat{A}_i d\hat{\sigma}_A, \qquad (i = 3,4),$$

$$F_i^{pp}(C) = \{G(x_1) f_f^p(x_2) \hat{A}_i - \Delta G(x_1) \Delta f_f^p(x_2) \hat{B}_i\} d\hat{\sigma}_C, \qquad (i = 3,4).$$

3. Electroweak Models and the Parametrizations

There is a nontrivial class of left-right models in which the lowest-mass gauge boson Z_1^0 is indistinguishable in mass and fermion couplings from the standard Z^0, but which allows a second gauge boson Z_2^0 as low as 200 GeV [see Ref. 3]. In such a left-right model the vector and axial-coupling constants of the lepton ℓ (quark f) to the Z_i^0-boson ($i = 1,2$), a_i^ℓ and b_i^ℓ (a_i^f and b_i^f) are expressed as follows:

For $i = 1$ (the lighter gauge boson Z_1^0), one has the standard model values:

$$\begin{aligned} a_1^\ell &= x_L - \frac{1}{4}, \\ b_1^\ell &= -\frac{1}{4}, \qquad for \quad \ell = e, \mu, \quad \text{and} \quad \tau, \end{aligned} \tag{2.18a}$$

and

$$\begin{aligned} a_1^f &= \frac{1}{2} I_3^f - e_f x_L, \\ b_1^f &= \frac{1}{2} I_3^f, \end{aligned} \tag{2.18b}$$

where I_3^f is the third component of the left-handed weak isospin of the quark, e_f is the charge of the quark f divided by the electric charge e, and $x_L = e^2/g_L^2 = \sin^2\theta_W$ with θ_W being the Weinberg angle.

For $i = 2$ (the heavier gauge boson Z_2^0), one has

$$\begin{aligned} a_2^\ell &= (x_L/x_R)^{1/2}(1 - x_L - x_R)^{-1/2}\{-\frac{1}{4}(1 - x_L + x_R) + x_R\}, \\ b_2^\ell &= \frac{1}{4}(x_L/x_R)^{1/2}(1 - x_L - x_R)^{1/2}, \qquad for \quad \ell = e, \mu, \quad \text{and} \quad \tau. \end{aligned} \tag{2.19a}$$

$$a_2^f = (x_L/x_R)^{1/2}(1-x_L-x_R)^{-1/2}\{\frac{1}{2}I_3^f \cdot (1-x_L+x_R) - e_f x_R\},$$
$$b_2^f = -(x_L/x_R)^{1/2}(1-x_L-x_R)^{1/2} \cdot \frac{1}{2}I_3^f, \tag{2.19b}$$

where $x_R = e^2/g_R^2$ [g_R being the $SU(2)_R$ coupling constant] is the parameter which characterizes the properties (mass, width, fermion coupling...) of the Z_2^0. A gauge-group-dependent parameter C_i within the left-right model we consider is given as:

$$C_1 = C_2 = e x_L^{-1/2}(1-x_L)^{-1/2}. \tag{2.19c}$$

In our numerical calculations we employ the standard model as well as the left-right model with the following parameters which reproduce the standard values at $Z = Z_1^0$, with three fermion generations, i.e., $N_f = 6$:

$$x_L = 0.233, \qquad x_R = 0.5,$$
$$M_{Z_1} = 93 \quad \text{GeV}, \qquad M_{Z_2} = 200 \quad \text{GeV}, \tag{2.20}$$
$$\Gamma_{Z_1} = 2.87 \quad \text{GeV}, \qquad \Gamma_{Z_2} = 3.77 \quad \text{GeV}.$$

As the parton spin distribution functions in the longitudinally polarized proton we employ the ones of Carlitz- Kaur(plus gluon) model, according to which the (spin) distributions of the u and d quarks read as:[20]

$$f_u^p(x) = u_v + \bar{u},$$
$$f_d^p(x) = d_v + \bar{d}, \tag{2.21a}$$

where

$$\bar{u}(x) = \bar{d}(x) = \frac{0.6}{x} \cdot (1-x)^{10},$$

$$\Delta f_u^p(x) = f_{u(+)}^{p(+)}(x) - f_{u(-)}^{p(+)}(x) = (u_v - \frac{2}{3}d_v)\cos 2\theta,$$
$$\Delta f_d^p(x) = f_{d(+)}^{p(+)}(x) - f_{d(-)}^{p(+)}(x) = -\frac{1}{3}d_v \cos 2\theta, \tag{2.21b}$$

with a spin dilution factor

$$\cos 2\theta = \{1 + 0.052x^{-1/2}(1-x)^2\}^{-1}. \tag{2.21c}$$

The sea-quark component is assumed to be unpolarized, i.e.,

$$\Delta f_{\bar{u}}^p(x) = \Delta f_{\bar{d}}^p(x) = 0. \tag{2.22}$$

The spin distribution of the gluon inside the proton has been estimated as follows,[21] assuming that the sea quarks are unpolarized and that the polarized gluons are emitted from the polarized valence quarks due to the QCD bremsstrahlung:[22]

$$G(x) = \frac{1.97}{x}(1-x)^6\{1 + (1-x)^2\},$$
$$\Delta G(x) = G_+^+(x) - G_-^+(x) = 0.43(2-x)(1-x)^6. \tag{2.23}$$

For the (scale-violating) distributions of the valence quarks inside the proton[23] :$u_v = u_v(x, Q^2)$ and $d_v = d_v(x, Q^2)$, we employ the ones by Glück, Hoffmann, and Reya,[24] taking as the scale of QCD evolution, $Q^2 = M^2$ =invariant mass squared of the lepton pair. For the QCD coupling constant α_s we use

$$\alpha_s(Q^2) = \frac{12\pi}{33 - 2N_f}\frac{1}{\ln Q^2/\Lambda^2}, \tag{2.24}$$

with $N_f = 6$ and $\Lambda = 0.4$ GeV which has been used in the fits of Ref. 24.

4. Numerical Results

As an application of the formulas discussed in Sections 2 and 3, we present in this Section the numerical results for the dileptons produced in $\bar{p}p_h$-collision at $\sqrt{s} = 540$ GeV as well as in $p_h p_h$-collision at $\sqrt{s} = 2$ TeV. In order to get as large as possible cross-section, we carry out the integration over the rapidity y of the dilepton in the range $-\ln 2/\bar{x}_T \leq y \leq \ln 2/\bar{x}_T$ which is obtained from the kinematical condition[14]

$$(x_1 - \frac{1}{2}\bar{x}_T e^y)(x_2 - \frac{1}{2}\bar{x}_T e^{-y}) = \frac{x_T^2}{4}, \tag{3.1}$$

where $\bar{x}_T = \sqrt{x_T^2 + 4\tau}$, $x_T = 2Q_T/\sqrt{s}$, and $\tau = M^2/s$. In the calculation Q_T of the dilepton is fixed at $Q_T = 5$ GeV. In some cases, we also present the results obtained by integrating over Q_T in the range $2 \leq Q_T \leq 12$ GeV (thereby introducing a cut-off in Q_T). Among various experimentally accessible coefficients in the angular distribution we will confine ourselves only to the parity-violating parameter α_1 which appears in the polar angle distribution[14]

$$\frac{dN}{d\cos\theta} = C(1 + \alpha_1 \cos\theta + \alpha_2 \cos^2\theta), \tag{3.2}$$

where

$$\begin{aligned} C =& \frac{3}{8}(1 + \frac{A_0}{2}), \\ \alpha_1 =& \frac{A_4}{1 + \frac{1}{2}A_0}, \qquad \alpha_2 = \frac{1 - \frac{3}{2}A_0}{1 + \frac{1}{2}A_0}, \end{aligned} \tag{3.3}$$

and present the results for the polarization asymmetry ΔA_4 given in Eqs.(2.15c) and (2.17c). Note that the curves for α_1, both in the standard and the left-right models change their sign in the Gottfried-Jackson (GJ-) frame as a function of

M near $M = M_{Z_i}$ on account of the L_f term, the interference between the γ^* and the Z_i^0-boson contributions.[14] One can take the advantage of this feature in determining Z_i^0-boson mass thereby testing the electroweak models. We present the numerical results for $\bar{p}p$-collision at $\sqrt{s} = 540$ GeV in Figs. 2-9 and for pp-collision at $\sqrt{s} = 2$ TeV in Figs. 10-13.

$\underline{\bar{p}p - \text{collision} \quad \text{at} \quad \sqrt{s} = 540 \quad \text{GeV}}$

We show in Figs.2-4 the following curves for the differential cross-section:

Fig. 2: $d\sigma/dMdQ_T$ as a function of M in unpolarized $\bar{p}p$-collision at $Q_T = 5$ GeV within the framework of both the standard and the left-right models.

Fig. 3: $d\sigma/dMdQ_T$ for unpolarized $\bar{p}p$-collision as a function of Q_T in the left-right model at $M = M_{Z_1} = 93$ GeV and $M = M_{Z_2} = 200$ GeV.

Fig. 4: $d\sigma/dM$ for unpolarized $\bar{p}p$-collison as a function of M, calculated in the Drell-Yan model and the left-right model.

In Figs. 5-6 we present the curves for the asymmetry defined in Eq.(2.13).

Fig. 5: $\{d\sigma(-) - d\sigma(+)\}/\{d\sigma(-) + d\sigma(+)\}$ as a function of M, for $\bar{p}p_h$-collision at $Q_T = 5$ GeV within the framework of the standard and the left-right models, where $d\sigma(\pm) = d\sigma(\pm)/dMdQ_T$.

Fig. 6: $\{d\sigma(-) - d\sigma(+)\}/\{d\sigma(-) + d\sigma(+)\}$ as a function of M, for $\bar{p}p_h$-collision within the framework of the standard and the left-right models, where $d\sigma(\pm) = \int_2^{12} dQ_T d\sigma(\pm)/dMdQ_T$. This quantity has been calculated also in Ref.[25] using the Drell-Yan model within the framework of the standard model.

The curves for the polarization asymmetry of the coefficient ΔA_4 under different conditions are shown in Figs. 7-9:

Fig. 7: ΔA_4 as a function of M, for $\bar{p}p_h$-collision at $Q_T = 5$ GeV, calculated in the GJ-frame within the framework of the standard and the left-right models.

Fig. 8: ΔA_4 as a function of M, for $\bar{p}p_h$-collision, integrated over Q_T in the range $2 \leq Q_T \leq 12$ GeV and calculated in the GJ-frame within the framework of the standard and the left-right models.

Fig. 9: ΔA_4 as a function of Q_T, for $\bar{p}p_h$-collision at $M = M_{Z_1} = 93$ GeV and $M = M_{Z_2} = 200$ GeV, calculated in the GJ-frame within the framework of the left-right model.

$pp-$collision at $\sqrt{s} = 2$ TeV

In Figs. 10-12 we display the curves for the differential and the integrated cross-sections:

Fig. 10: $d\sigma/dMdQ_T$ as a function of M for unpolarized pp-collision at $Q_T = 5$ GeV within the framework of both the standard model and the left-right models.

Fig. 11: $d\sigma/dMdQ_T$ for unpolarized pp-collision as a function of Q_T in the left-right model at $M = M_{Z_1} = 93$ GeV and $M = M_{Z_2} = 200$ GeV.

Fig. 12: $\int_2^{12} dQ_T d\sigma/dMdQ_T$ as a function of M, calculated within the framework of the left-right model, for unpolarized pp-collision.

The polarization asymmetry of the cross-section defined in Eq.(2.16a): $\{d\sigma(--) - d\sigma(++)\}/\{d\sigma(--) + d\sigma(++)\}$ is shown in Fig. 13 as a function of M, for doubly polarized $p_h p_h$-collision, calculated within the framework of the standard and the left-right models, where $d\sigma(\pm\pm) = \int_2^{12} dQ_T d\sigma(\pm\pm)/dMdQ_T$.

Before concluding this section let us make a few remarks.

1. The predictions by the standard model cannot be discriminated from the ones by the left-right model near to $M \simeq M_{Z_1}$. The difference between

the two models starts to appear only in $M \gtrsim 150$ GeV,and becomes most prominent in the region $M \simeq M_{Z_2}$.

2. The shapes of the curves in Figs. 5, 7 with fixed $Q_T (= 5$ GeV) are very similar to the ones of the curves in Figs. 6, 8 correspondingly in which Q_T is integrated over in the region $2 \leq Q_T \leq 12$ GeV, but the absolute values differ slightly.

3. The asymmetry of the coefficient ΔA_4 (shown in Figs. 7, 8, and 9), calculated in the GJ-frame, almost coincides with the one calculated in the Collins-Soper (CS-) frame.[26] The ΔA_4 in the helicity frame differs somewhat from the one in the GJ-frame, taking smaller absolute values.

4. The asymmetries for the other coefficients $\Delta A_i (i = 0 - 3)$ appear to be rather small in all the three (helicity, GJ-, and CS-) reference frames.

5. Although we have ignored the sea-quark polarization, it can be shown that these effects are rather small.[27] This is not the case for the effects of gluon radiation which are important[27] , but which were not considered here for sake of simplicity.

6. When the beam energy increases the polarization effects seem to decrease. Existing calculations also indicate such tendency.[7] which was also observe in the case of W production.[27] This fact suggests that polarized beam experiments at uitra high energies, say, at $\sqrt{s} = 100$ TeV are not very encouraging.

5. Conclusion

As one can see from the figures presented in the previous Section the measurements of polarization asymmetries of the coefficients in the angular distribution using the polarized proton beams, which would constitute a "complete" experiment, would provide us with a variety of detailed information about different underlying electroweak gauge models, their couplings and thereby would allow to distinguish and verify such models. In particular the sign of the asymmetries is related to the structure of the underlying gauge theory. Besides, the polarized beam reactions could shed light on the production mechanism, such as reconfirmation of the vector nature of a gluon, and the spin distributions of the partons inside hadrons as well.

We conclude this paper by stressing that experimentation with the high-energy polarized proton beams with a sufficiently high luminosity accessible at the CERN $\bar{p}p$ collider and the Fermilab Tevatron would provide a powerful tool of investigation, complementing the ones obtainable in the unpolarized experiments, and might exploit new rich realm of "spin" physics.

ACKNOWLEDGEMENTS

Two of the authors (M. H. and K. Y.) would like to thank Professor S. D. Drell and the other members of the Theory Group for their warm hospitality at SLAC. We also thank H. Aoyama for useful help in preparing the manuscript. This work was supported by the U.S. Department of High Energy under contract number DE-AC03-76SF00515.

REFERENCES

1. S. Weinberg, *Phys. Rev. Lett.* **19** (1967) 1264;
   A. Salam, *Proc. of the 8-th Nobel Symposium*, edited by N. Svartholm (Almqvist and Wiksell, Stockholm 1968) p.36;
   S.L. Glashow, *Nucl. Phys.* **22** (1961) 579.
2. G. Arnison et al.(UA1 collaboration), *Phys. Lett.* **B122** (1983) 103;
   M. Banner et al. (UA2 collaboration), *Phys. Lett.* **B122** (1983) 476;
   G. Arnison et al. (UA1 collaboration), *Phys. Lett.* **B126** (1983) 398;
   M. Banner et al. (UA2 collaboration), *Phys. Lett.* **B129** (1983) 130.
3. V. Barger, E.Ma, and K.Whisnant, *Phys. Rev.* **D28** (1983) 1618 and references quoted therein.
4. H. Georgi, in *Particle and Fields*-1974, edited by C. E. Carlson, AIP Conference Proceedings No. 23 (American Institute of Physics, New York, 1975);
   H. Fritzsch and P. Minkowski, *Ann. Phys. (N.Y.)* **93** (1975) 193.
5. H. S. Mani and S.D. Rindani, *Phys. Lett.* **84B** (1979) 104.
6. F. E. Paige, T. L. Trueman, and T.N.Tudron, *Phys. Rev.* **D19** (1979) 935;
   F. E. Paige; Proc. Topical Workshop on Production of New Particles in Super-High Energy Collisions, edited by V. Barger and F. Halzen, University of Wisconsin, Madison, 1979.
7. R. Kinnunen and J. Lindfors, *Nucl. Phys.* **B189** (1981) 63;
   J. Lindfors; AIP Conference Proceedings **95** (1983) 259 (Editor G. Bunce).
8. K. Hidaka, *Nucl. Phys.* **B192** (1981) 369.

9. J. Soffer: Proc. of the SPS Fixed Target Workshop held at CERN (1982); CERN Yellow Report 83-02 Vol. II p.392 (Editor I. Mannelli);
See also, N. S. Craigie, K. Hidaka, M. Jacob, and F.M. Renard, *Phys. Rep.* **99** (1983) 69.

10. H. E. Haber and G. L. Kane, *Nucl. Phys.* **B146** (1978) 109;
F. E. Paige et al., in Ref.5.

11. For the calculation based on the standard model, see M. Hayashi, S. Homma, and K. Katsuura, *J. Phys. Soc. Jpn.* **50** (1981) 1427;
J. Finjord, G. Girardi, M. Perrottet, and P. Sorba, *Nucl. Phys.* **B182** (1981) 427;
P. Aurenche and J. Lindfors, *Nucl. Phys.* **B185** (1981) 301;
I. H. Dumbar and N. Dombey, *Phys. Lett.* **101B** (1981) 197;
D. J. E. Callaway, *Ann. Phys.(N.Y.)* **144** (1982) 282.
See also Ref. 13.

12. T.G. Rizzo, *Phys. Rev.* **D27** (1983) 1075.

13. G. Girardi, P. Mery, and P. Sorba, *Z. Phys.* **C10** (1981) 363.

14. M. Chaichian, M. Hayashi, and K. Yamagishi, *Phys. Rev.* **D25** (1982) 130, *ibid.* **D26** (1982), 2534 (E).

15. N.S. Craigie,T.Niinikoski, A. Penzo, L. Van Rossum, R. D. Ruth L. Sivers, and J. Soffer, Saclay Report, D. Ph. PE 83-01 (1983).

16. M. Chaichian, O. Dumbrajs, and M. Hayashi, *Phys. Rev.* **D20** (1979) 2873;
F. Halzen and D. M. Scott, *Phys. Lett.* **78B** (1978) 318;
J. Finjord et al., in Ref. 10;
P. Aureche and J. Lindfors, *Nucl. Phys.* **B185** (1981) 274.

17. M. Chaichian, M. Hayashi, and K. Yamagishi, Trieste preprint IC/83/33 (1983).

18. K. Hagiwara, K. Hikasa, and N. Kai, *Phys. Rev. Lett.* **52** (1984) 1076.

19. N. Arteaga-Romero, A. Nicolaidis and J. Silva, *Phys. Rev. Lett.* **52** (1984) 172.

20. R. Carlitz and J. Kaur, *Phys. Rev. Lett.* **38** (1977) 673, *ibid.* **38** (1977) 1102 (E); J. Kaur, *Nucl. Phys.* **B128** (1977) 219.

21. F. Close and D. Sivers, *Phys. Rev. Lett.* **39** (1977) 1116. See also J. Ralston and D. Soper, *Nucl. Phys.* **B152** (1979) 109.

22. G. Altarelli and G. Parisi, *Nucl. Phys.* **B126** (1977) 298.

23. For a more complete analysis of scaling violation of the spin dependent structure function, see P. Chiappetta and J. Soffer , Preprint CPT-84/p. 1615, to appear in Phys. Rev. **D**.

24. M. Glück, E. Hoffmann, and E. Reya, *Z. Phys.* **C13** (1982) 119.

25. P. Aurenche and J. Lindfors in Ref. 10.

26. J.C. Collins and D. E. Soper, *Phys. Rev.* **D16** (1977) 2219.

27. P. Chiappetta and J. Soffer, Preprint CPT-84/p.1650, to appear in Phys. Lett. **B**.

Figure Captions

1. (a) The quark-antiquark annihilation diagrams.

   (b) The quark-gluon Compton diagrams.

2. The differential cross-section $d\sigma/dMdQ_T$ vs M for unpolarized $\bar{p}p$-collision at $\sqrt{s} = 540$ GeV and $Q_T = 5$ GeV. The dashed (solid) curve corresponds to the standard (left-right) model.

3. The differential cross-section $d\sigma/dMdQ_T$ vs Q_T, calculated in the left-right model, for unpolarized $\bar{p}p$-collision at $\sqrt{s} = 540$ GeV, $M = M_{Z_1} = 93$ GeV and $M = M_{Z_2} = 200$ GeV. The curve shown for $M = M_{Z_2} = 200$ GeV is multiplied by 10^2 to the actual values.

4. The differential cross-section $d\sigma/dM$ vs M for unpolarized $\bar{p}p$-collision at $\sqrt{s} = 540$ GeV, calculated within the framework of the Drell-Yan model assuming the left-right model.

5. The asymmetry, $\{d\sigma(-) - d\sigma(+)\}/\{d\sigma(-) + d\sigma(+)\}$ vs M for $\bar{p}p_h$-collision at $\sqrt{s} = 540$ GeV and $Q_T = 5$ GeV, where $d\sigma(\pm) = d\sigma(\pm)/dMdQ_T$. The dashed (solid) curve corresponds to the one calculated within the framework of the standard (left-right) model.

6. The asymmetry, $\{d\sigma(-) - d\sigma(+)\}/\{d\sigma(-) + d\sigma(+)\}$ vs M for $\bar{p}p_h$-collision at $\sqrt{s} = 540$ GeV, where $d\sigma(\pm) = \int_2^{12} dQ_T d\sigma(\pm)/dMdQ_T$. The dashed (solid) curve is the prediction by the standard (left-right) model.

7. The asymmetry of the coefficient ΔA_4 vs M for $\bar{p}p_h$-collision at $\sqrt{s} = 540$ GeV and $Q_T = 5$ GeV, calculated in the GJ-frame. The dashed (solid) curve is the prediction by the standard (left-right) model.

8. The asymmetry of the coefficient ΔA_4, integrated over Q_T in the range

$2 \leq Q_T \leq 12$ GeV, for $\bar{p}p_h$-collision at $\sqrt{s} = 540$ GeV, shown as a function of M in the GJ-frame. The dashed (solid) curve is the prediction by the standard (left-right) model.

9. The asymmetry of the coefficient ΔA_4 vs $Q_T$for $\bar{p}p_h$-collision at $\sqrt{s} = 540$ GeV, $M = M_{Z_1} = 93$ GeV and $M = M_{Z_2} = 200$ GeV, calculated in the GJ-frame using the left-right model.

10. The differential cross-section $d\sigma/dMdQ_T$ vs M for unpolarized pp-collision at $\sqrt{s} = 2$ TeV and $Q_T = 5$ GeV. The dashed (solid) curve is the prediction by the standard (left-right) model.

11. The differential cross-section $d\sigma/dMdQ_T$ vs Q_T, for unpolarized pp-collision at $\sqrt{s} = 2$ TeV, $M = M_{Z_1} = 93$ GeV and $M = M_{Z_2} = 200$ GeV, calculated in the left-right model.

12. $\int_2^{12} dQ_T d\sigma/dMdQ_T$ as a function of M, calculated within the framework of the left-right model, for unpolarized pp-collision.

13. The asymmetry, $\{d\sigma(--) - d\sigma(++)\}/\{d\sigma(--) + d\sigma(++)\}$ vs M for doubly polarized $p_h p_h$-collision at $\sqrt{s} = 2$ TeV, calculated within the framework of both the standard (dashed curve) and the left-right (solid curve) models, where $d\sigma(\pm\pm) = \int_2^{12} dQ_T d\sigma(\pm\pm)/dMdQ_T$.

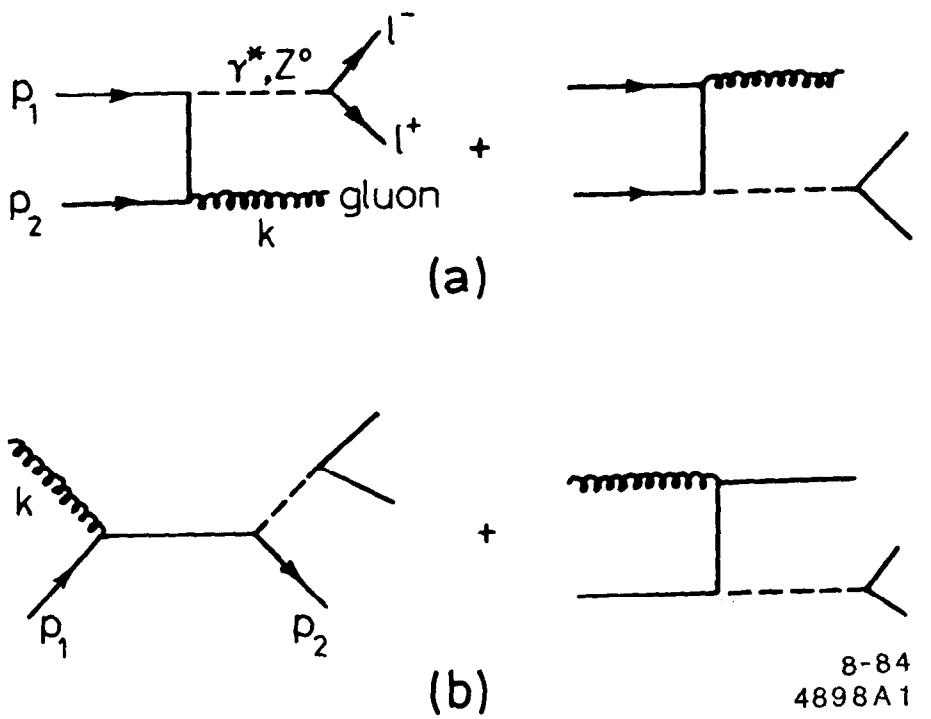

Fig. 1

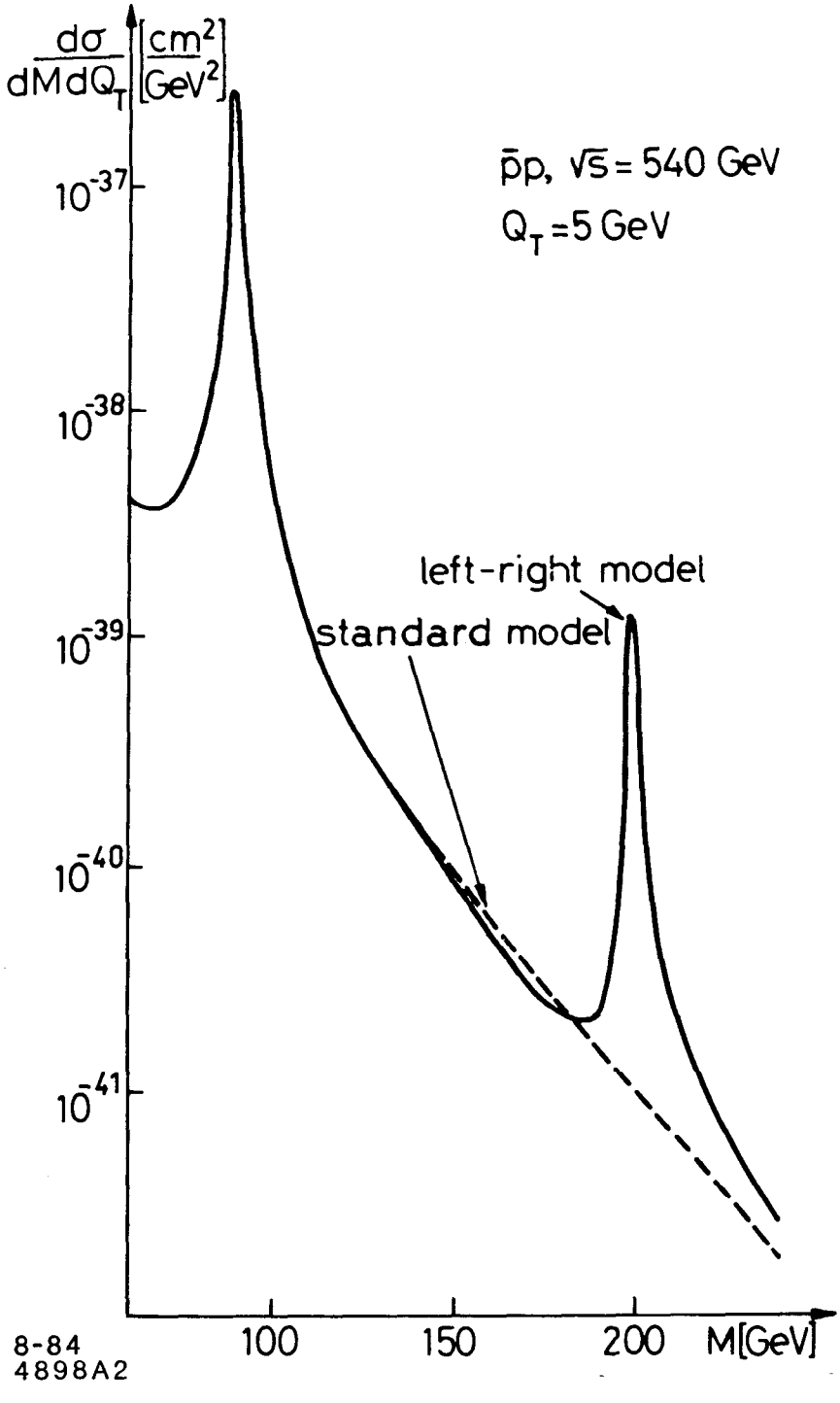
$\frac{d\sigma}{dMdQ_T}\left[\frac{cm^2}{GeV^2}\right]$
$\bar{p}p$, $\sqrt{s}$ = 540 GeV
Q_T = 5 GeV
10^{-37}
10^{-38}
10^{-39}
10^{-40}
10^{-41}
left-right model
standard model
100
150
200
M[GeV]
8-84
4898A2

Fig. 2

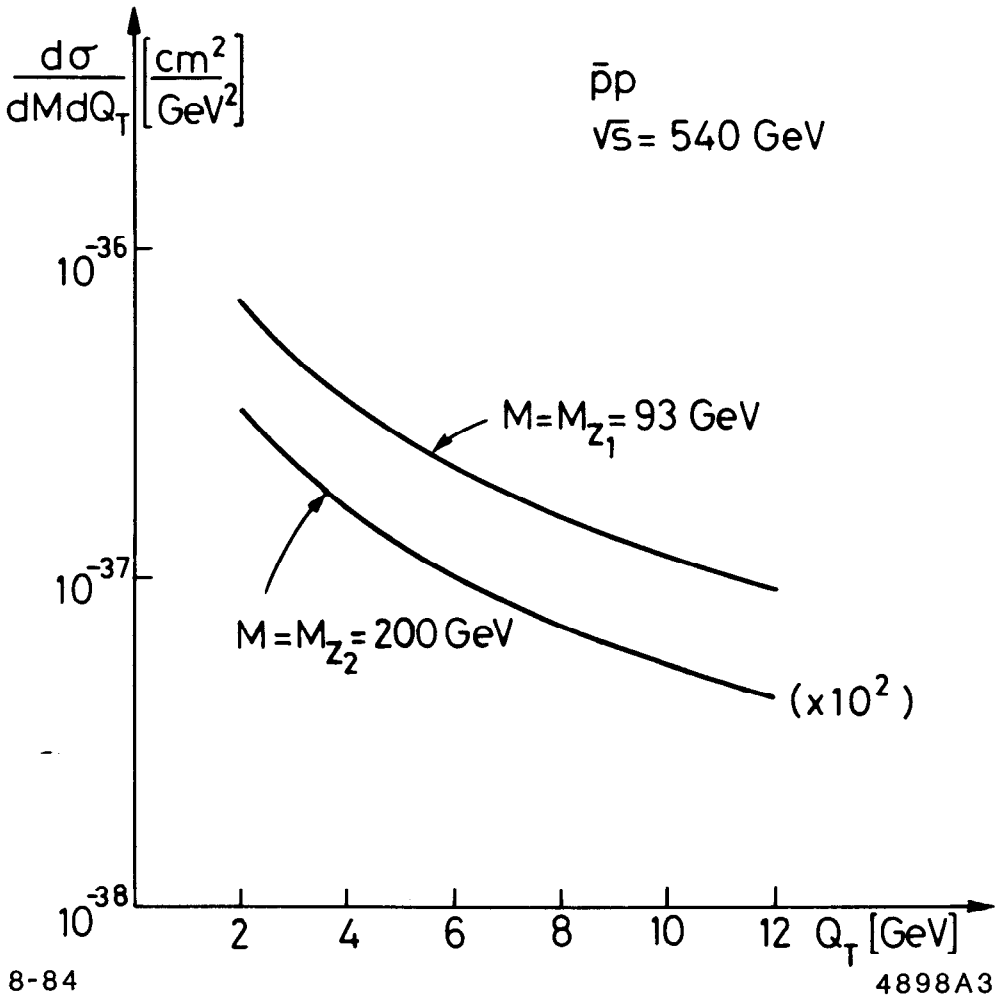
dσ/dMdQ_T [cm²/GeV²]
p̄p
√s = 540 GeV
10^-36
10^-37
10^-38
M=M_Z1=93 GeV
M=M_Z2=200 GeV
(x10²)
2
4
6
8
10
12
Q_T [GeV]
8-84
4898A3

Fig. 3

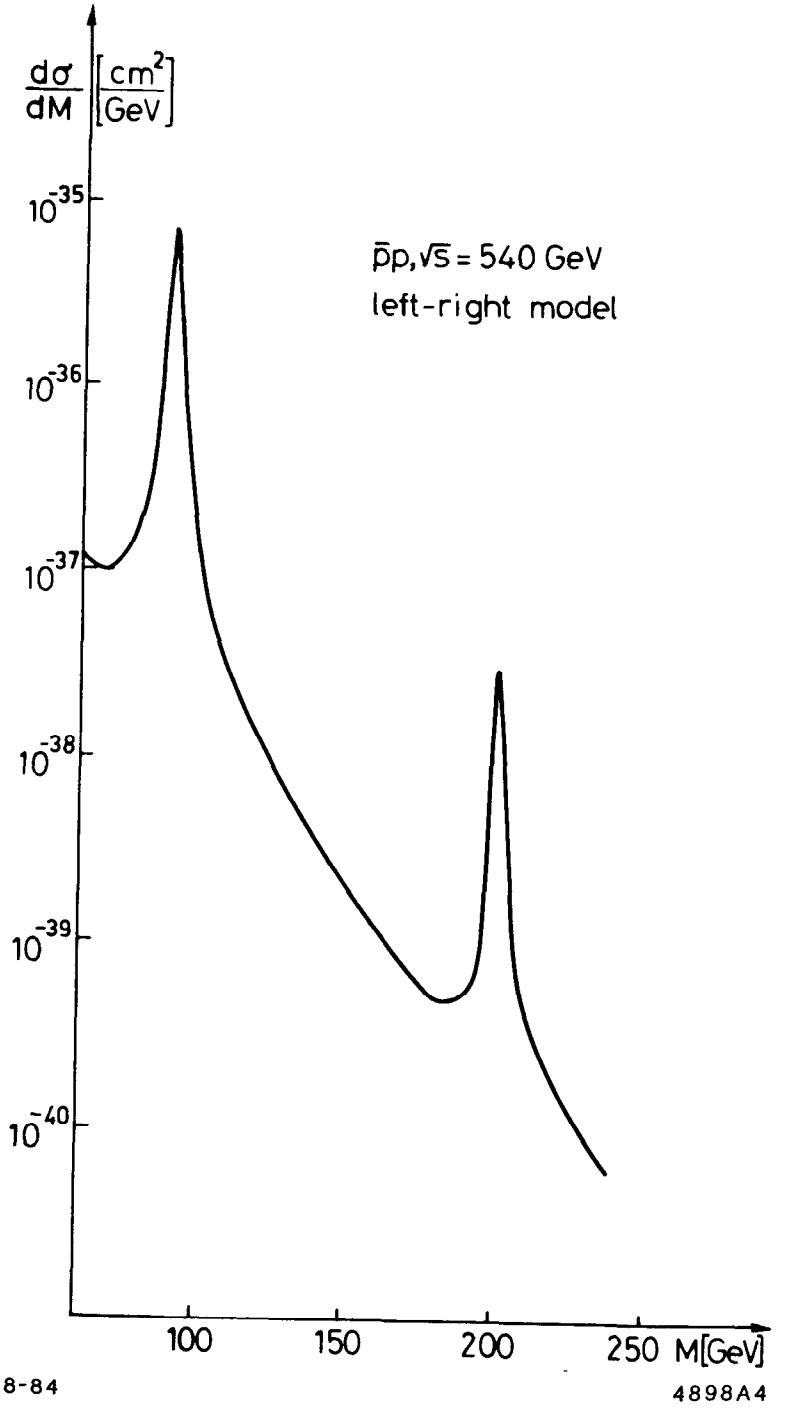
dσ/dM [cm²/GeV]
10⁻³⁵
10⁻³⁶
10⁻³⁷
10⁻³⁸
10⁻³⁹
10⁻⁴⁰
p̄p, √s = 540 GeV
left-right model
100
150
200
250 M[GeV]
8-84
4898A4

Fig. 4

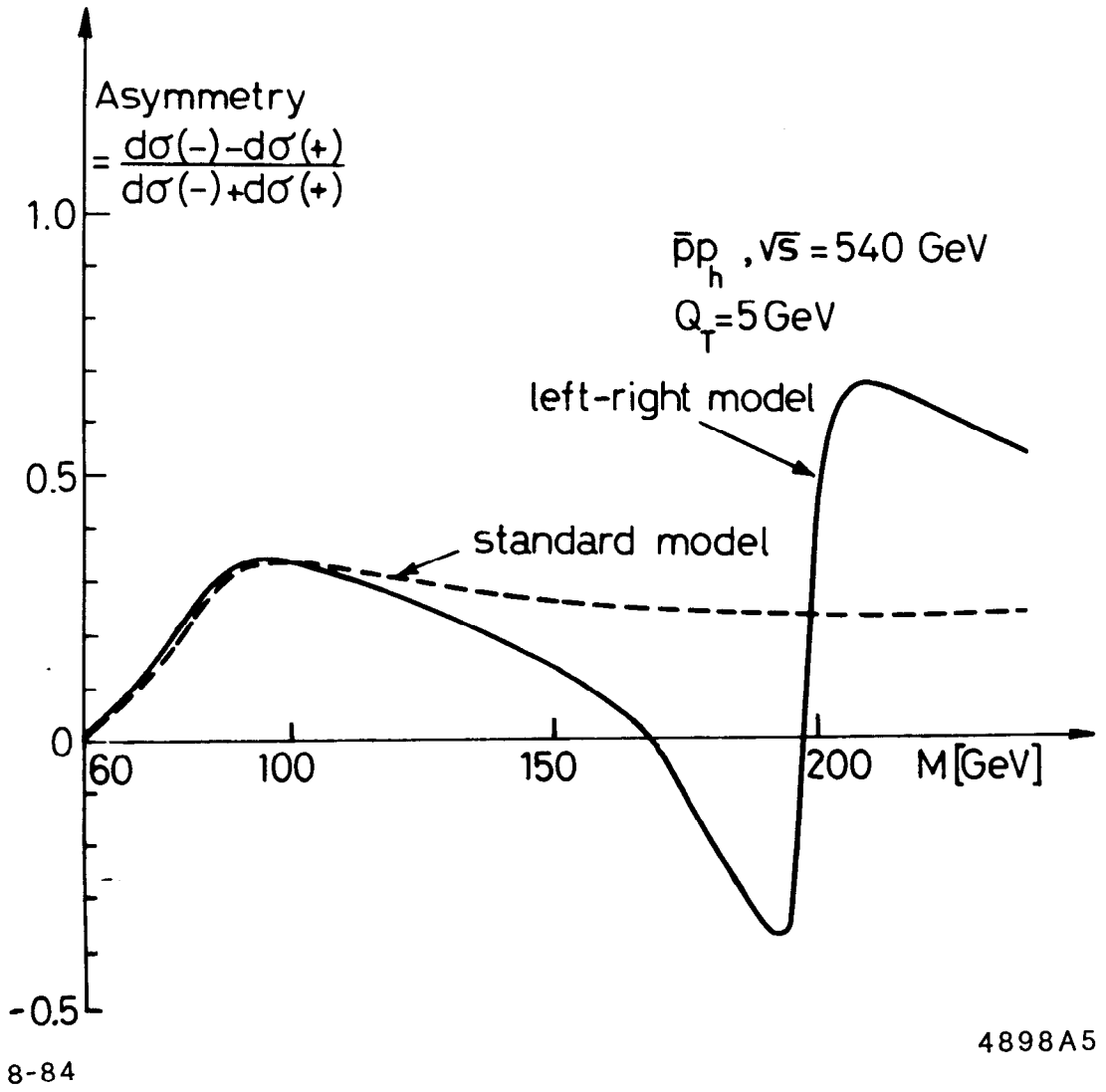
Asymmetry
= dσ(−)−dσ(+) / dσ(−)+dσ(+)
1.0
0.5
0
-0.5
$\bar{p}p_h$, $\sqrt{s}$ = 540 GeV
Q_T = 5 GeV
left-right model
standard model
60
100
150
200
M[GeV]
4898A5
8-84

Fig. 5

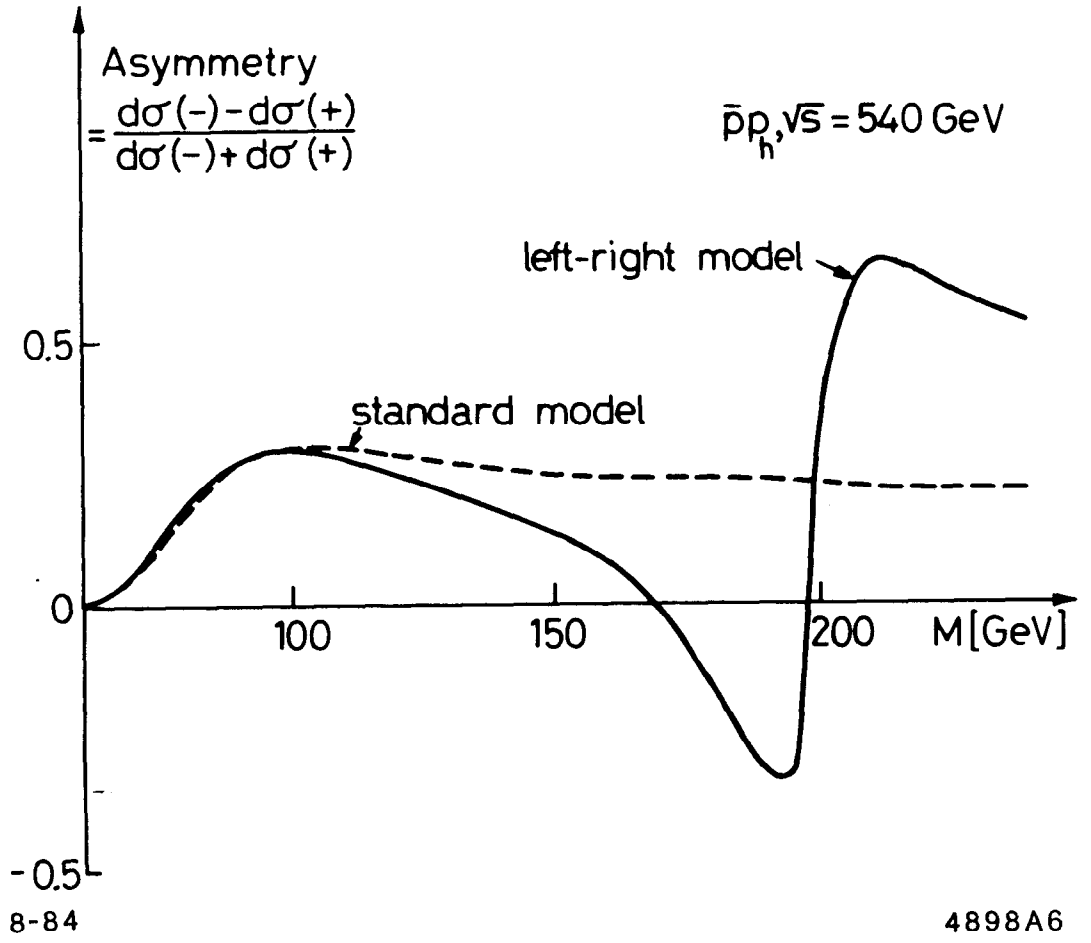
Asymmetry
$= \frac{d\sigma(-) - d\sigma(+)}{d\sigma(-) + d\sigma(+)}$
$\bar{p}p_h, \sqrt{s} = 540$ GeV
left-right model
standard model
0.5
0
-0.5
100
150
200
M[GeV]
8-84
4898A6

Fig. 6

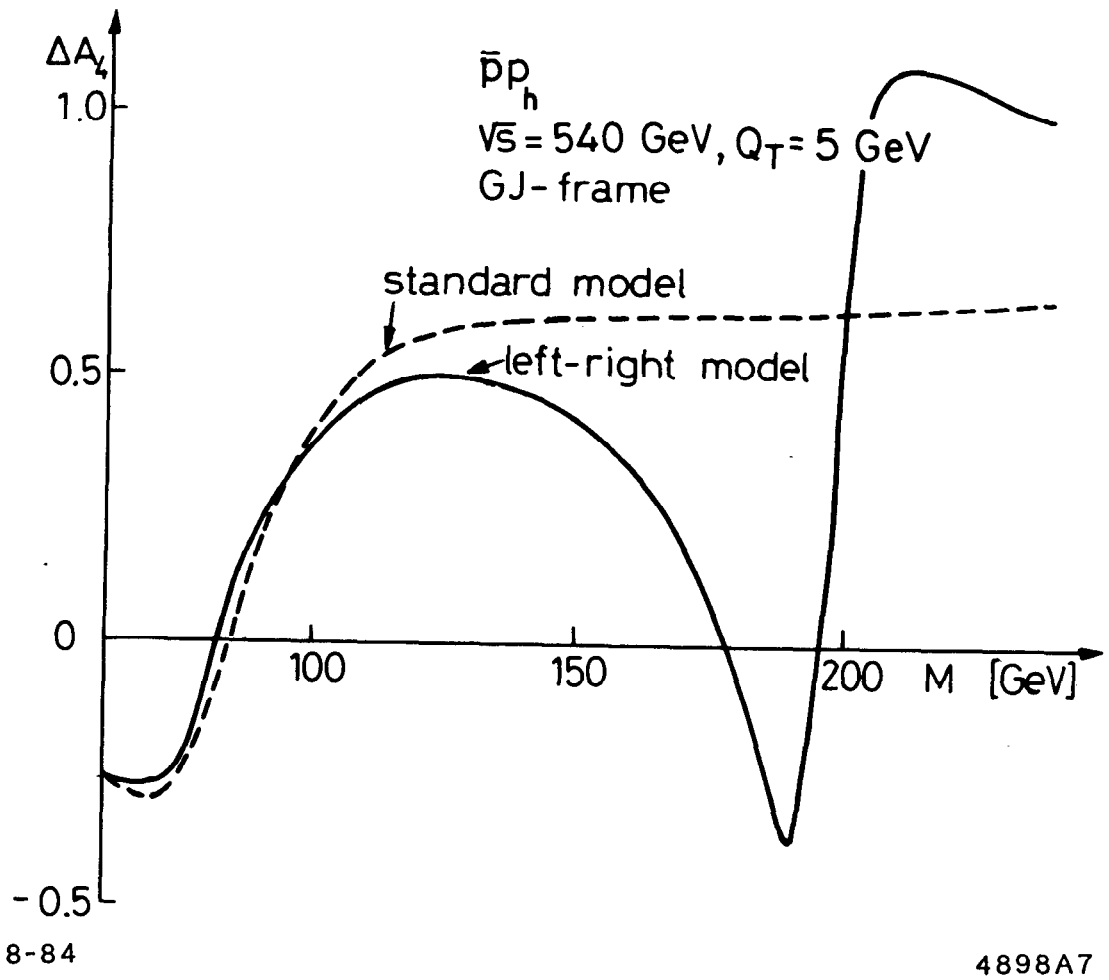
ΔA4
1.0
0.5
0
-0.5
p̄p h
√s = 540 GeV, QT = 5 GeV
GJ-frame
standard model
left-right model
100
150
200
M [GeV]
8-84
4898A7

Fig. 7

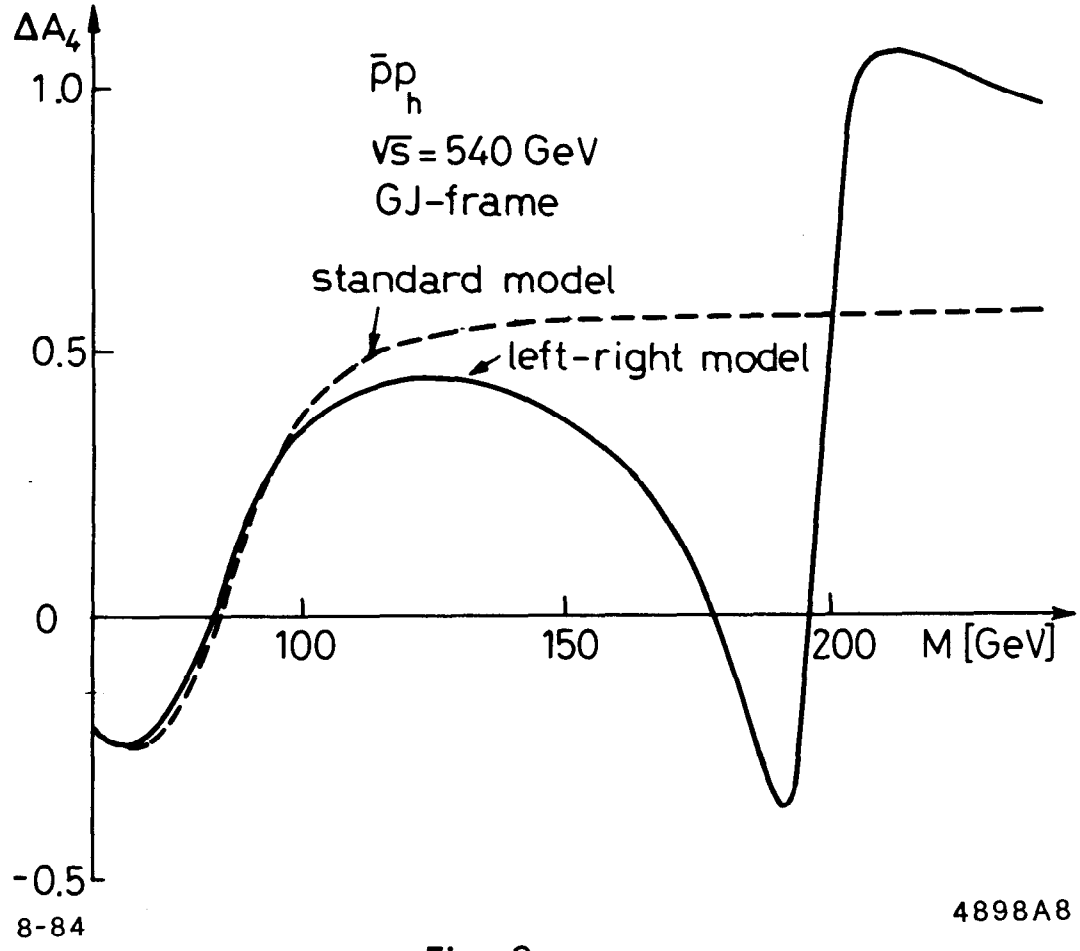
ΔA4
1.0
0.5
0
-0.5
p̄ph
√s = 540 GeV
GJ-frame
standard model
left-right model
100
150
200
M [GeV]
8-84
4898A8

Fig. 8

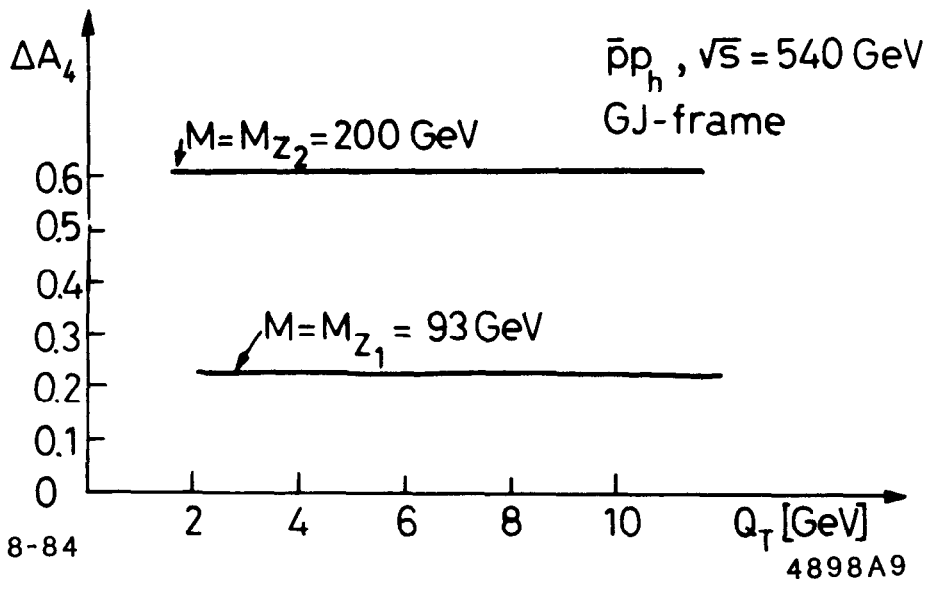
ΔA4
p̄ph , √s = 540 GeV
GJ-frame
M=MZ2=200 GeV
M=MZ1 = 93 GeV
0.6
0.5
0.4
0.3
0.2
0.1
0
2
4
6
8
10
QT [GeV]
8-84
4898A9

Fig. 9

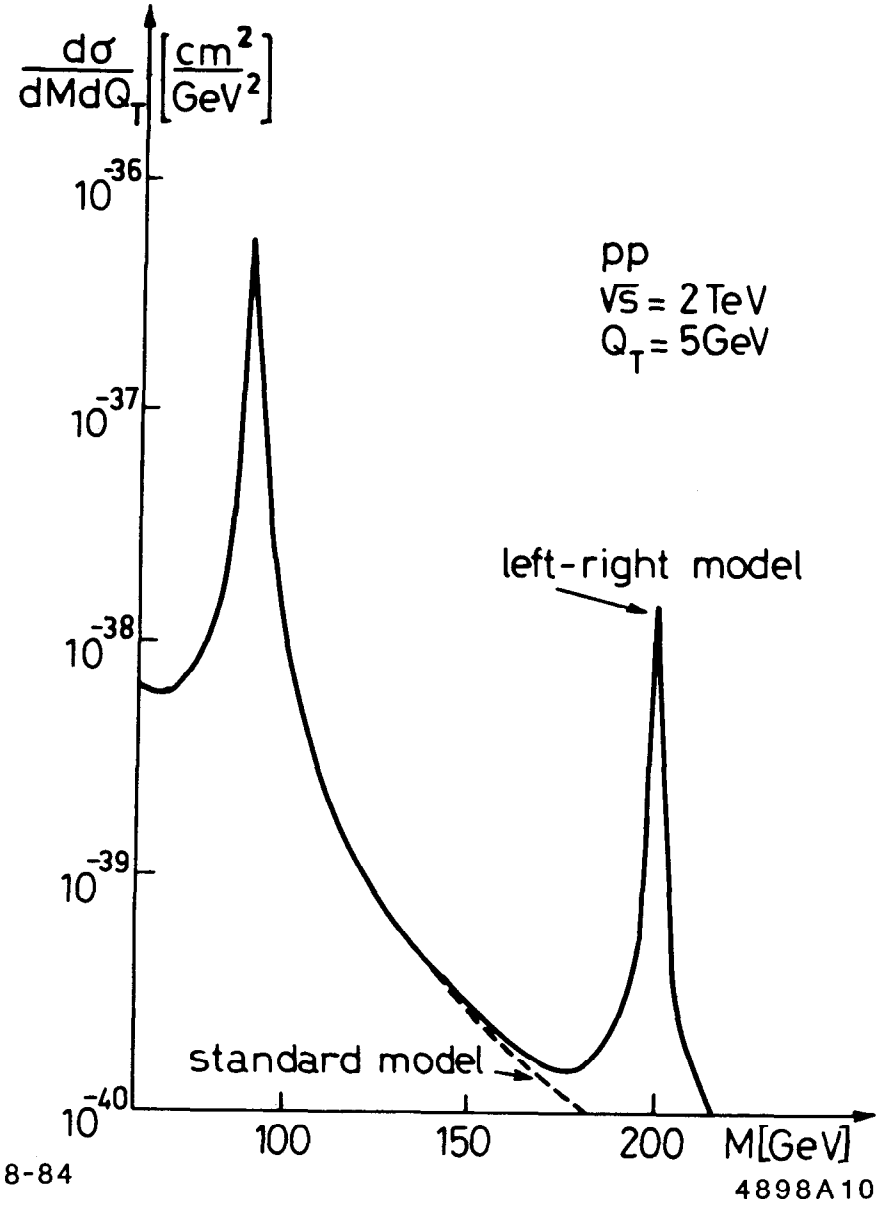
dσ/dMdQ_T [cm²/GeV²]
10^-36
10^-37
10^-38
10^-39
10^-40
pp
√s = 2 TeV
Q_T = 5GeV
left-right model
standard model
100
150
200
M[GeV]
8-84
4898A10

Fig. 10

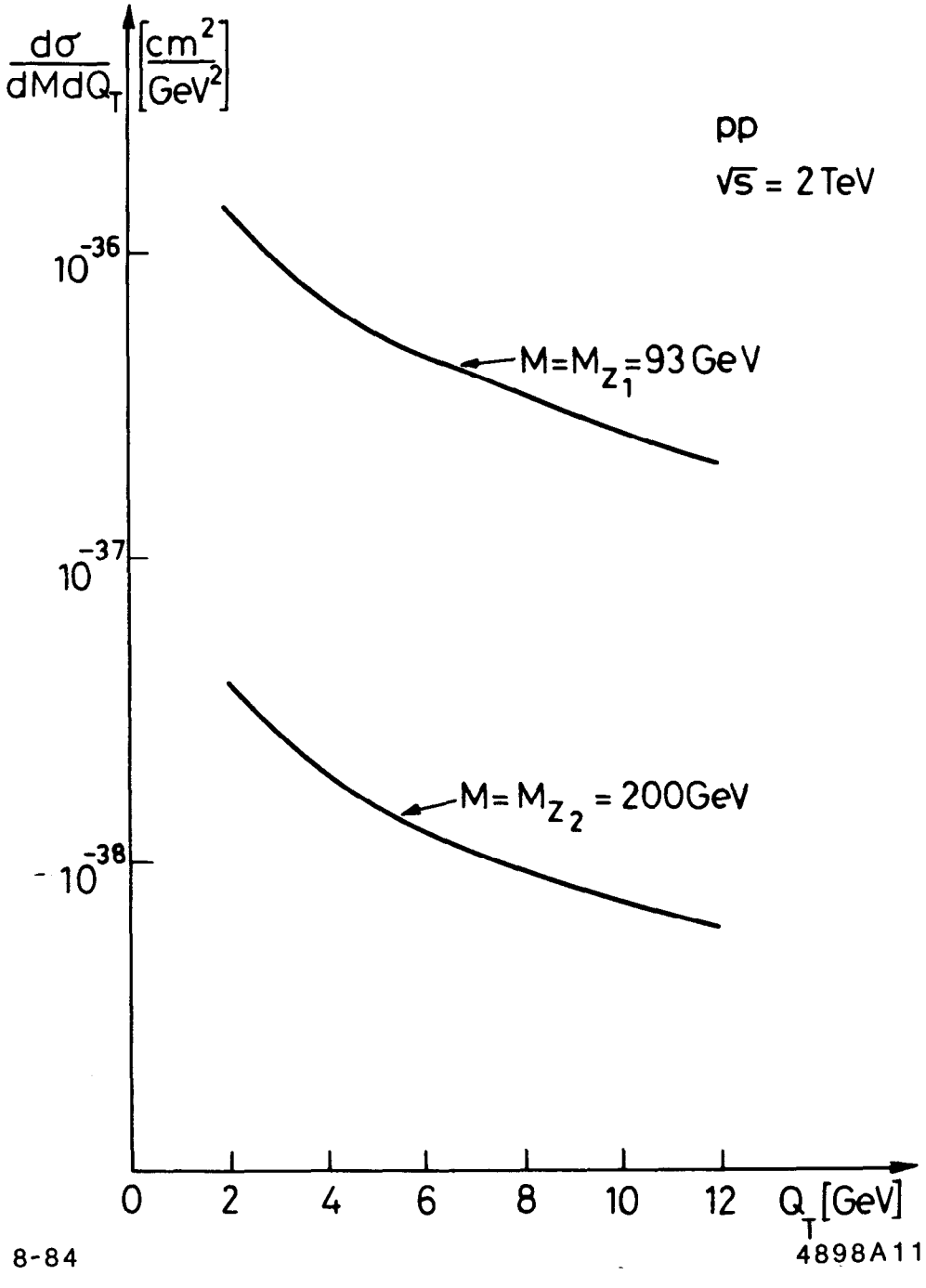
dσ/dMdQ_T [cm²/GeV²]
pp
√s = 2 TeV
10^-36
10^-37
10^-38
M=M_Z1=93 GeV
M=M_Z2 = 200GeV
0
2
4
6
8
10
12
Q_T [GeV]
8-84
4898A11

Fig. 11

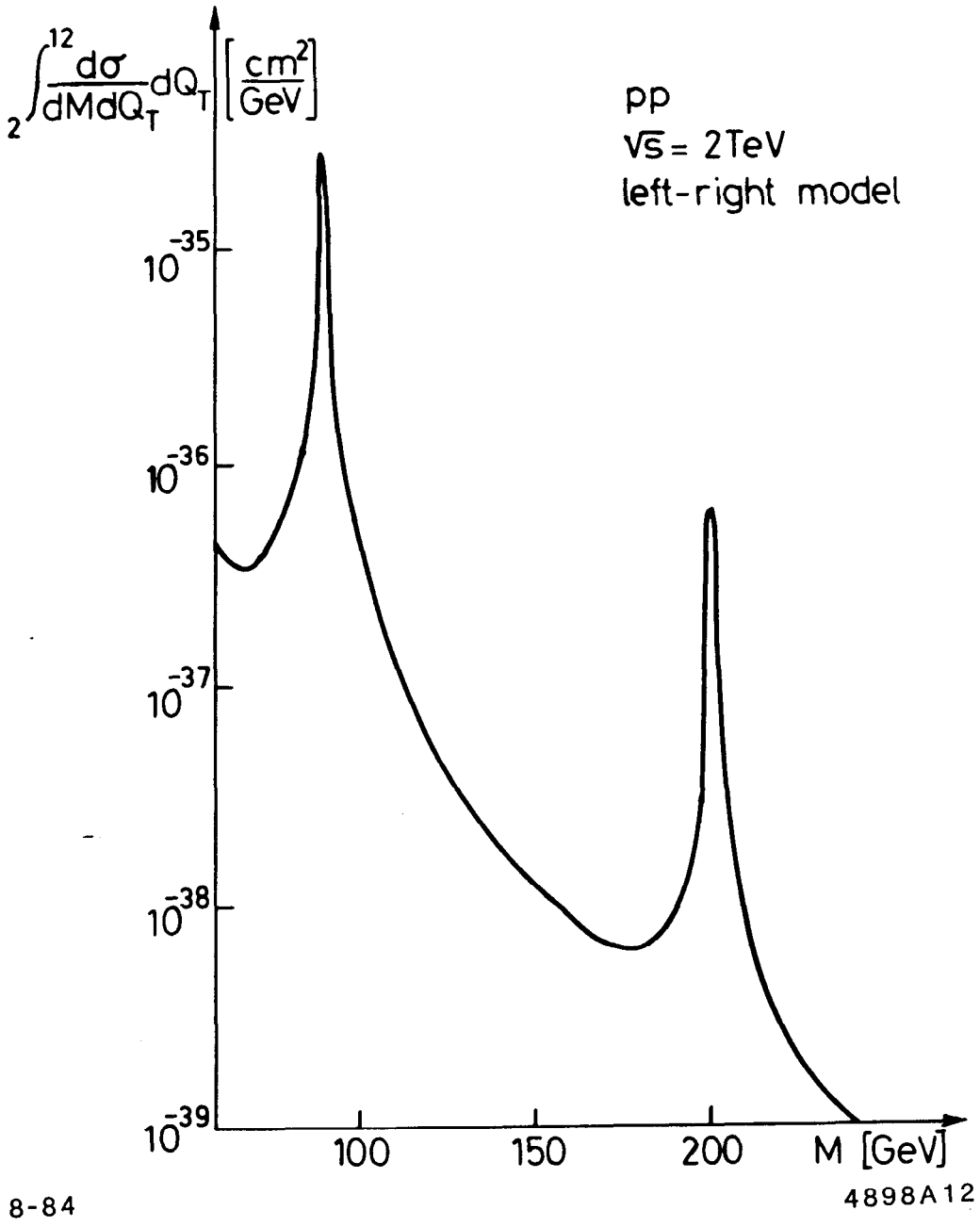
$\int_2^{12} \frac{d\sigma}{dM dQ_T} dQ_T \left[\frac{cm^2}{GeV}\right]$
pp
$\sqrt{s}$ = 2TeV
left-right model
10^{-35}
10^{-36}
10^{-37}
10^{-38}
10^{-39}
100
150
200
M [GeV]
8-84
4898A12

Fig. 12

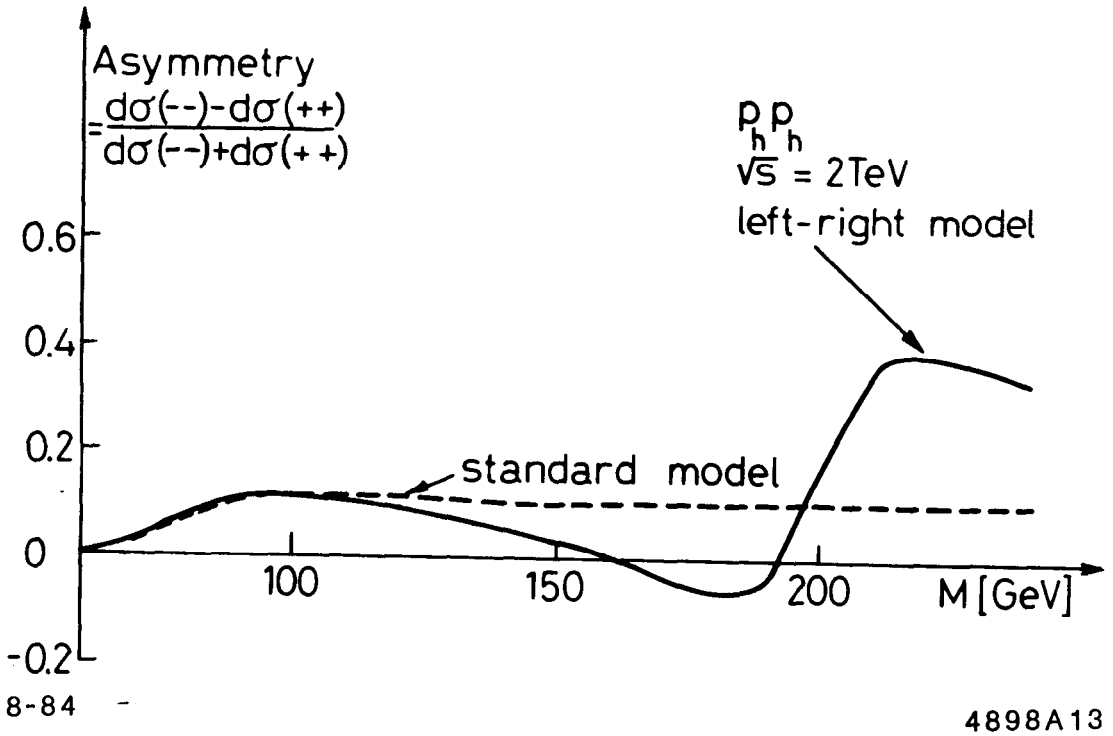
Asymmetry
$=\frac{d\sigma(--)-d\sigma(++)}{d\sigma(--)+d\sigma(++)}$
$p_h p_h$
$\sqrt{s}$ = 2TeV
left-right model
standard model
0.6
0.4
0.2
0
-0.2
100
150
200
M [GeV]
8-84
4898A13

Fig. 13